IMECE2021-73235

MODELING DISCHARGE SPARK IGNITION USING ZERO DIMENSION THERMODYNAMIC MODEL AND EXPERIMENTAL POWER MEASUREMENTS AT VARIOUS PRESSURES

James Shaffer West Virginia University Morgantown, WV Saeid Zare Mississippi State University Starkville, MS Omid Askari West Virginia University Morgantown, WV

ABSTRACT

Laminar burning speed calculation at high pressures is challenging because of unstable surface conditions at large flame kernel diameters. It is therefore desired to take these measurements at small dimensions (i.e., during and immediately after the ignition discharge process) when the flame kernel is smooth and stable. Taking accurate measurements at these sizes is challenging because the kernel growth rate does not only depend on the chemical reaction but also on other phenomena such as energy discharge, as well as radiative and conductive energy losses. The effect of these events has not been adequately assessed, due to the generation of ionized gas (i.e., plasma). In order to better understand the effect of the ignition plasma in this work, spark ignition in air for 1-5 atm of pressure is studied. Understanding the ignition event and modeling its behavior is important to capture accurate combustion measurements at pressures pertinent to the advanced high-pressure engines and technologies. The relationship between the electrical energy supplied to the spark and the thermal energy dissipated within a gas mixture has been studied. This work relates the electrical discharge power to the volume of the ignition kernel measured via schlieren imagery. Voltage and current data are also captured as the input to a thermodynamic model which is used to predict the volume versus time data of the spark event. The model, which utilizes measured electrical power, thermodynamic properties of ionized air, and radiation losses in air show agreement with the experimental kernel measurements in terms of overall shape of the volume data within the measured kernel uncertainty. With these results and further experimental validation the present model is considered to represent the relationship between the electrical spark power and the measured ignition kernel volume. Future work will be done to determine inaccuracies present in the arc discharge regime as well as the effectiveness of the model in combustible media.

Keywords: Ignition, Glow Plasma, Arc Plasma, Atmospheric Discharge, High Pressure, Modeling

1. INTRODUCTION

Fundamental experimental measurements of laminar burn speed at high pressures are challenging to measure because at large radius the flame surface becomes cellular from instabilities. Works such as Al-Shahrany et al. [1] utilize two flame surfaces and a relation to describe characterize the instabilities with regards to the peclet number to correct the measured cellular burn speed to the laminar burn speed. This method however will still be dependent on the accuracy and quality of the Peclet number in order to perform the correction. The uncertainty of which increases at higher pressures. Development of an alternative method to measure high pressure laminar burn speeds is desired and will take data at radius prior to the formation of instabilities. One of the major issues preventing the use of data in this range, aside from the high stretch and curvature affects, is the affect spark ignition has on the flame. For this reason, the goal of this work is to document and measure the effect that the spark ignition has on the measured schlieren kernel in order to support future combustion diagnostics.

Three different plasma formations: breakdown, glow and arc discharge (discussed in more detail in Section 3) are observed experimentally in the spark discharge. The model outlined in section 2 focuses on the glow discharge as the plasma structure is more easily measurable in schlieren imaging than arc discharge, however, the model can still be applied to arc discharge. The breakdown plasma is neglected in the model as the as the effect on the kernel size is minimal.

Spark discharge models such as one provided in Kim and Anderson [2] give a great description of the plasma structure and energy deposition to the surrounding atmosphere for engine relevant conditions. This work is great for understanding how spark energy is converted into thermal energy (within the bulk plasma) and non-thermal energy (within the cathode sheath region). However, the modeling work done estimates the bulk velocity of the gas rather than quantifying the thermal affect ignition has on the air and combustion. Since the goal of this work is to relate plasma discharge energy to the schlieren size and shape of the kernel, results from Kim and Anderson ignition

model do not provide enough precision in the time and position domain. Work by Sher et al [3] provides a detailed description of the breakdown stage of the ignition process. Breakdown, which is not considered for the model, is experimentally minimized in this work through the reduction of the spark gap resulting in breakdown energy smaller than 1mJ with small effects on the schlieren kernel. Venkattraman et al. Kolobov et al. and Sommerer et al. [4–6] all propose models to describe cathode and anode fall voltages for similar conditions used in this work. The cathode and anode sheath structures are formed around the cathode and anode electrodes to separate the bulk plasma from the electrode. These sheaths are formed from positive ions and in the DC plasma pulse in this work is most strongly formed about the cathode. the energy used in the formation of these structures is the primary nonthermal loss mechanisms in the ignition event. While good for estimation, these relations that describe the cathode fall voltage depend on several gas parameters and work function of the electrode material. The work function can change depending on the surface structure of the electrode [7] and having accurate gas parameters for the specific gas compositions and pressures will be challenging. Because of this experimental measurement of cathode fall is considered for more accuracy with methodology of measurement discussed in a separate work also similar methods to Hao et al. [8]. Uhrlandt et al. [9] likewise considers cathode and anode fall models for arc discharge which is only briefly considered in this work. Because the surface area of the electrode covered in arc plasma is far less than the area encompassed by glow discharge the total cathode and anode fall is greatly reduced but with the results presented here are still relevant. Maly [10] has also created a model to describe the ignition process, however, the goal for Maly's research is to describe minimum ignition energy and how the plasma ignites the flame. As a result, the conclusions in Maly's work are not necessarily useful for the goals of this research. Maly's ignition model describes the minimum ignition energy in terms of how the temperature of the ignition manifests spatially with respect to time, but this model does not provide radius vs time data desired in this research. Kim and Anderson [2] come close to describing the plasma in a way that is relevant to this research, however, the relationship between the input electrical energy and the size of the ignition is not developed. While the velocity proposed in this work could be integrated to find the positional data it would not take into account the affect temperature has on the kernel size and an accurate expression of electric field can be challenging to calculate.

The model that is presented in this work will show the relationship between the electrical power supplied to the plasma and the schlieren volume or radius of the ignition kernel. The measured electrical data should only represent the thermal energy added to the spark gap. Separate research measures and considers energy loss within the plasma structure to be the

cathode fall. This claim will also be considered in the results presented

2. IGNITION MODEL

The ignition model governing equation Eq. 1 considers the change in kernel volume to be a combination of the measured spark power \dot{SE} which is the thermal spark energy previously mentioned minus the radiation losses. This work will use the NEC radiation data [11] for air and will not consider the conductive losses. The power term is related to the change in volume through the multiplied relation in Eqn. 1 where T represents the temperature of the plasma mixture, R is the gas constant, P is the pressure, P0 is the specific heat and P0 is the specific gas constant. Each property changes with temperature where appropriate (mass and pressure are constant). These thermodynamic properties of the plasma are calculated with the method detailed by Askari et al [12,13].

$$\frac{dV}{dt} = \left(\frac{R}{pc_p} + \frac{T\Omega}{pc_p}\right) \left(\dot{SE} - \dot{Q}_{rad}\right) \tag{1}$$

Spark power, \dot{SE} , already considers electrical and plasma inefficiencies as shown in Eq. 2 and discussed in more detail in a separate work where the circuit losses are associated with resistive inefficiencies and are experimentally excluded through the selection of voltage measurement location. The cathode fall loss is the power dissipated across the cathode sheath where the voltage drop is across the cathode sheath is measured and used to correct the measurement during glow discharge.

$$\dot{SE} = P(t)_{Measured} - P(t)_{Cathodefall} - P(t)_{Circuitlosses}$$
 (2)

Alternatively, the change in radius, assuming a spherical kernel, can also be calculated utilizing Eq. 3 where A is the surface area of the kernel.

$$\frac{dr}{dt} = \left(\frac{R + T\Omega}{Apc_p}\right) \left(\dot{SE} - \dot{Q}_{rad}\right) \tag{3}$$

While both Eqs. 1 and 3 can be used to calculate the model radius and volume of the ignition kernel these equations assume some knowledge of temperature which is not experimentally known in this work and must be solve computationally. To solve for temperature, the computation is separated into two steps where the change in temperature is found for each time step as shown in Eq. 4.

$$\frac{dT}{dt} = \left(\frac{1}{mc_p}\right) \left(\dot{SE} - \dot{Q}_{rad}\right) \tag{4}$$

The volume of the kernel can then be found utilizing the newly found temperature and considering the density of the gas mixture at the new temperature. If an experimental temperature is captured the model could utilize Eqs. 1 or 3 directly.

Originally the inputs of the model were the initial volume, the initial temperature, and the measured electrical data. However, it was found to be challenging to measure a starting volume and temperature with enough precision at this small scale (immediately after breakdown) in order to pose a well-defined system resulting in inaccurate solutions. A different method is

needed to define the mass and initial temperature for this work until more experimental data is captured (such as temperature) to define the system better.

Because of this, the inputs of the model are the measured electrical power, the initial temperature, the final temperature and the final radius. The final temperature and final radius are used to define the mass of the system and with the initial temperature and mass the initial volume is found. Using the mass and Eq. 4 the state of the kernel at the next data point can be found. Because the final temperature is unknown the program is repeated until the guess final temperature and the calculated final temperature converge. A flow chart of model routine is provided in Fig. 1.

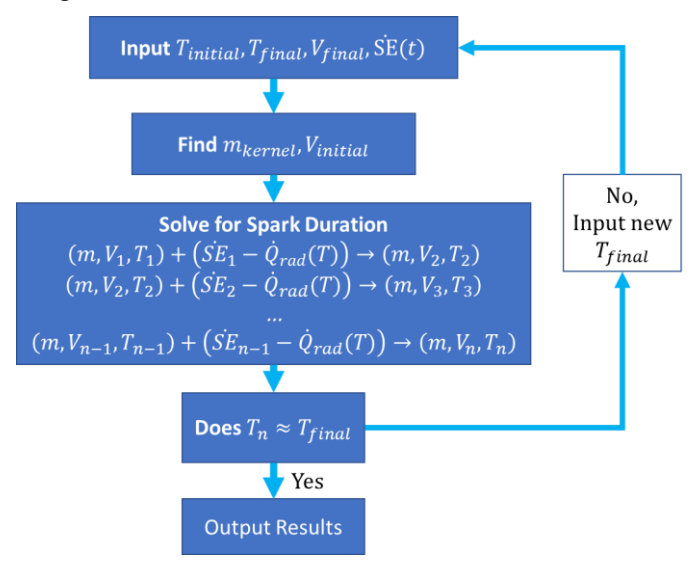


FIGURE 1: FLOW CHART OF PLASMA MODEL ROUTINE

The initial temperature is currently an unknown value estimated to be near ambient temperature immediately following breakdown. While the temperature of the breakdown event is hot (>6000K), it is suspected, based off the propagation of the plasma kernel, that immediately after breakdown there is some initial mass growth that cools the kernel to very low temperatures (near ambient). Other researchers such as Kawahara [14] typically use systems which provide electrical currents that initially start at high currents after breakdown and decay over the spark pulse. which should change the temperature profile of the plasma. In contrast, the plasma observed experimentally in this work starts with nearly zero current after breakdown and has a parabolic shape, which, in addition to a mass gain, results in the low initial temperature. All temperatures are considered to be averaged spatially over the schlieren kernel as part of the LTE condition.

The assumptions on which the model operates are listed:

- 1. Ideal gas,
- 2. The kernel has a constant mass,
- 3. The kernel has a constant pressure,
- 4. Local thermodynamic equilibrium (LTE).

3. THE SPARK KERNEL AND PLASMA

The spark discharge is initiated by breakdown, which is then followed by either, glow plasma for the remainder of the process, or, followed by a glow-arc-glow transition depending on the current, pressure and electrode conditions. Figure 2 illustrates the spark process and shows the ionized gas region in solid color while the heated gas kernel region visualized in the schlieren images is shown with a dashed line. The model and model assumptions begin at the start of glow discharge in Fig. 1b once the glow plasma has stabilized. The growth from Fig. 1a to 1b is considered to have a significant mass gain as the ionized region expands across the surface of the high voltage electrode. After Fig. 1b, the kernel is considered to expand only with temperature change as energy is added to the system.

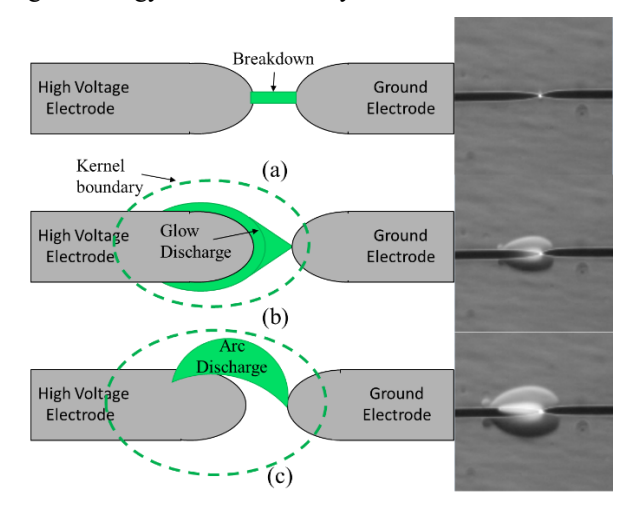


FIGURE 2: PROCESSES FOR IGNITION DISCHARGE INCLUDES (A) BREAKDOWN FOR INITIATING THE SPARK; (B) GLOW DISCHARGE WITH UNIFORM DISCHARGE OVER HIGH VOLTAGE ELECTRODE; (C) ARC DISCHARGE FROM POINT TO POINT.

Glow discharge is desired for its uniform current density about the axis of the electrode which results in symmetric kernels. If the spark discharged purely in arc mode, the resulting kernel would be erratic and will be challenging to measure with the methods shown in this work. this is because the arc discharge discharges between two spots which can change location during a single spark event. Rapid arc plasma movement can cause wrinkles and distortion in the ignition kernel if the kernel is not well established. If the kernel is well established from an initial glow plasma discharge such as in Fig. 2 small amounts of arc can occur without large distortions in the kernel. The best way to maintain glow discharge and prevent arc mode is keeping a clean, polished electrode surface.

The model of the glow discharge is shown in Fig. 3 where three structures within the ionized region cause potential drops across the spark gap. The cathode sheath causes a large non-thermal loss from the high electric field produced at the tip. This sheath is formed of positive ions and covers the surface of the electrode. The rest of the potential drop after the cathode sheath in the bulk

plasma and anode fall results in thermal collisions resulting in the majority of the heat production. A detailed analysis of nonthermal loss within the arc phase has not been experimentally investigated for the ignition system so the arc phase will initially be considered loss-less. After observing the full arc power in the results a loss equivalent in nature to the cathode fall in glow discharge estimated to be on the order of 10V-20V for arc will be considered. The values used are on the same order as those described in Kim and Anderson [2], Uhrlandt et al. [9] or Lichtenberg et al. [15]. For Cathode fall a value between 300V and 330V is used which is measured for atm air.

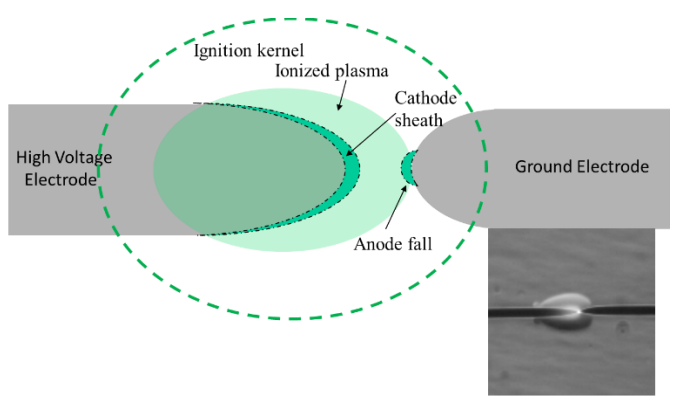


FIGURE 3: STRUCTURE OF THE GLOW PLASMA

The effect of pressure is also considered for this work. The ignition process can behave erratically at high pressure especially during arc plasma. The erratic behavior stems from the transition between glow and arc discharge and the rapid change in arc plasma location and size. The behavior arises from electrode instabilities associated surface (roughness/sharp edges). The plasma becomes more sensitive to these imperfections in the electrode as the pressure increases. With an electrode cleaning regimen involving polishing with up to 10k grit sandpaper, glow discharge could be achieved (without arc discharge) up to 5 atm however this condition is challenging to maintain. After 5 atm of pressure strong arcing is likely to occur, which at high pressure is likely to affect the surface requiring polishing to prevent heavy arcing. It should be noted the research is being developed to enhance fundamental laminar burn speed measurements. Because of this, accurate measurements are desired rather than more efficient or more energetic plasmas. As discussed previously glow discharge is symmetric about the electrodes which makes for more precise volume measurements. Alternatively arc discharge may convert the electrical energy into thermal energy more efficiently but can create wrinkles on the ignition kernel scale.

A sample of kernels in air over a range of initial pressures is shown in Fig. 4. The change in pressure results in a change in kernel size that is accounted for by using thermodynamic (in Eq. 4) and radiation data calculated for the experimental pressure used. While images at many different pressures are presented here model results will only be presented for 1, 3 and 5 atm.

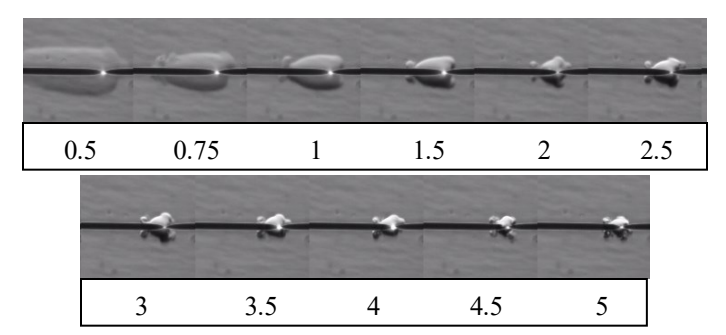


FIGURE 4: EFFECT OF PRESSURE ON KERNEL SIZE PRESSURE LABELED UNDER PICTURE IN ATM.

4. MATERIALS AND METHODS

4.1 Experimental Setup

The experimental setup is presented in two separate systems. The first is the electrical spark generation and measurement. The second is the visual Schlieren imaging system used to measure the volume of the affected gas.

4.2 Spark Generation and Measurement

The spark discharge is created by providing high voltage pulse to the spark gap initiated by passing a high current pulse through the primary windings of an automotive ignition coil. The result is sinusoidal current driven by a second order resistor inductor capacitor (RLC) circuit. By changing the initial stored voltage in the capacitor (150 uf), the magnitude of the current passed is changed. The secondary coil will see a current pulse on the order of 1 amp. The duration of the spark pulse is driven by the inductance and resistance of the ignition coil, a street fire 5527 automotive coil. The system is capable of producing multiple discharges with one signal; therefore, a diode system is used to suppress secondary discharge by passing the second discharge to ground with an avalanche diode system.

The voltage measurement is captured using a Northstar PVM-4 probe which has a 0.4% uncertainty, and the current is captured using a Pearson 6595 Current monitor which has a 1% uncertainty. The probe measurements are then captured using an NI-9222 four channels ADC which has 16 bits of vertical resolution and a sample rate of 500 kHz. The Pearson current coil data is affected by droop which causes the actual value of current to fall over the duration of the signal by some percentage of the value. This is corrected for by using Eq. 5 where i_{Meas} is the signal received by the device and τ is the characteristic time constant of the current coil.

$$i_{Correct} = i_{Meas} + \frac{\int i_{Meas}}{\tau}$$
 (5)

The voltage and current data captured is used to find power and energy which is found using Eqs. 6 and 7.

$$P(t)_{elec} = V(t) * I(t)$$
(6)

$$P(t)_{elec} = V(t) * I(t)$$

$$E(t)_{elec} = \int P(t) dt , E_{Total} = \int_{t_1}^{t_2} P(t) dt$$
(6)
(7)

4.3 Visual Images and Measurement

The volume of heated gas which is used to compare to the energy measurement is captured with Schlieren imaging. A Phantom V611 is used to capture the images. Typical setting uses a 128x128 pixel window with a 180k fps sample rate. The camera lens is a sigma DG 300mm model which provides a resolution between 10- 23 pxl/mm scale depending on the setings. The Schlieren system uses two Thorlabs Plano-convex lenses to manipulate a Thorlabs 700mW, 625nm wavelength LED light. A system schematic is shown in Fig. 5.

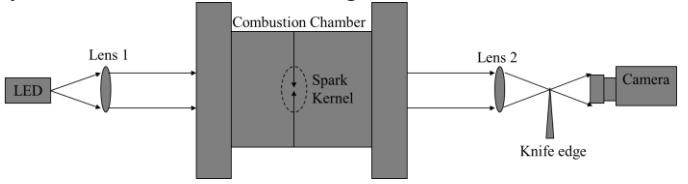


FIGURE 5: SCHLIEREN EXPERIMENTAL SETUP.

The combustion chamber is cylindrical and has a diameter and height of 5.25 inches and uses borosilicate glasses to provide visual access to the ignition kernel. A knife cuts the light horizontally at the focal point of the second lens to provide the Schlieren effect.

The measurement of the spark kernel involves post processing in phantom camera software PCC and in MATLAB to detect the upper edge of the kernel shown highlighted in Fig. 6 on the right image. The pixels within the detected edge are then revolved about the center of axis of the kernel to find the total volume. Only the measured kernel volume is presented in the results because the kernels are in general assumed only symmetric about the electrode and the model does not distinguish between the kernel shapes. In the future during a combustion event the added chemical energy will cause a more spherical shape at which point the volume of the model can be related to the radius of the sphere.

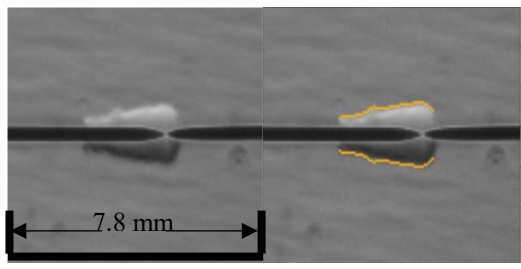


FIGURE 6: SAMPLE OF SCHLIEREN KERNEL EDGE DETECTION.

The uncertainty of the measured volume is found in two parts. First, the size of the pixel is considered and the change in volume for plus and minus a half pixel with is found for each data point. The second component of uncertainty shows how precise the edge detection is over time. For a spark kernel that follows a known function, the deviation from that function is found. To do this the derivative of the data is taken until the data is centered on zero. The standard deviation is found, and in this case, it is then scaled to the original volume by multiplying with dt^2 . An

example of this uncertainty calculation is shown in Fig. 7. The uncertainty of the final volume for this case is approximately $1.5 \, mm^3$. The uncertainty grows over the entire test because of the increasing number of pixels involved in taking the measurement.

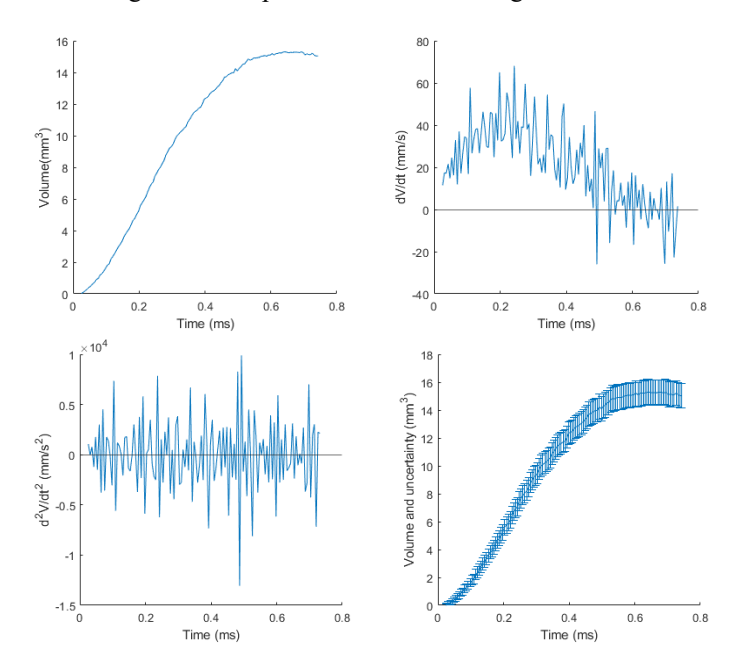


FIGURE 7: UNCERTAINTY FOR VOLUME DATA.

4.4 Experiments

The results will explore the accuracy of the model in air at 1 and 3 atm of pressure in air. Discharge with both arc and glow plasma in are utilized to show the robustness of the model prediction and to discuss the non-thermal loss within the arc discharge. Results for the first three conditions of Table 1 will show data with and without considing the cathode fall loss as it is desired to see the accuracy of the measured glow cathode fall studied in a separate work. Additional tests with only the final results are shown in the final entries.

TABLE 1: CONDITIONS FOR EXPERIMENTAL RESULTS PRESENTED.

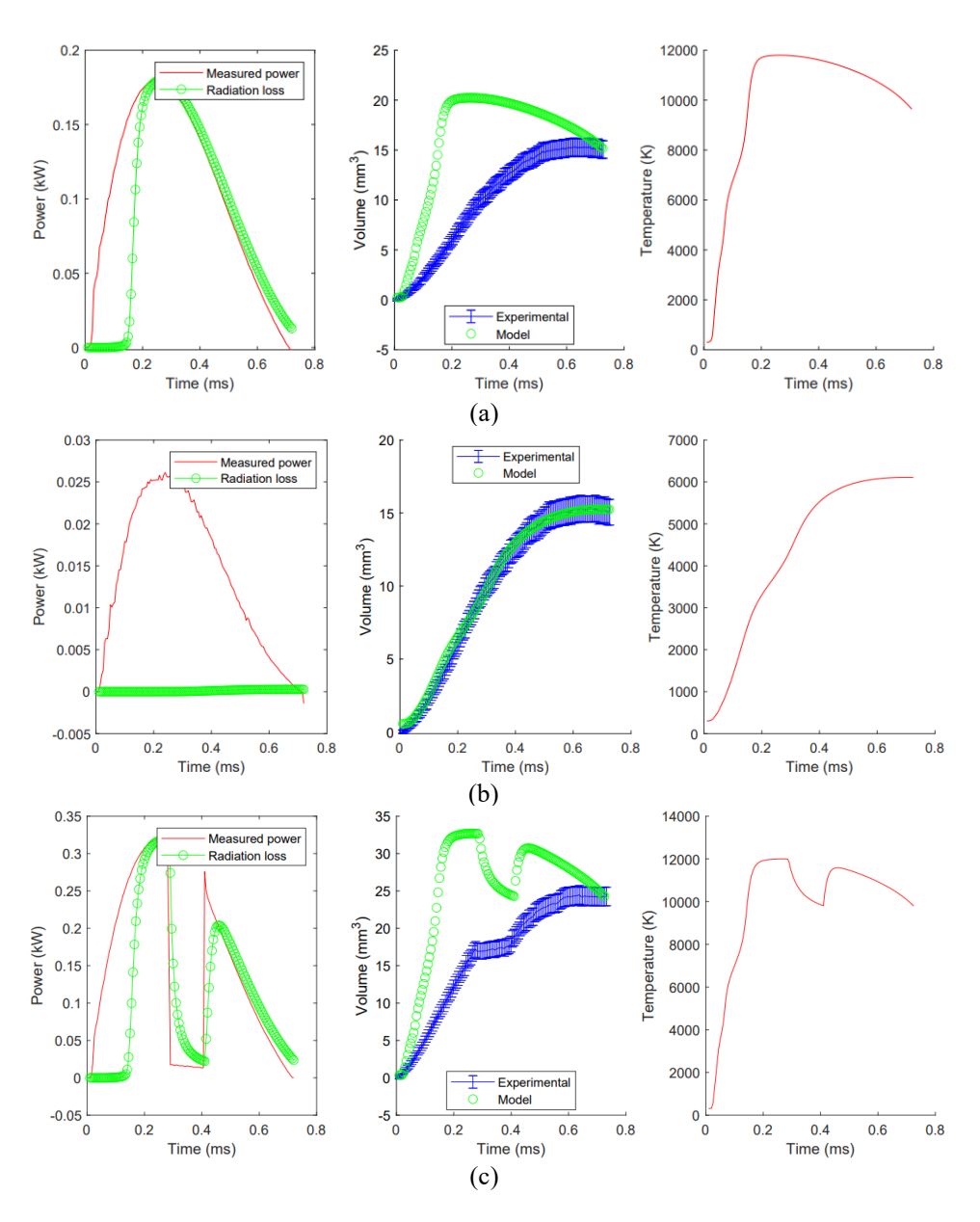
THE SELLIES TO THE SELECTION OF THE SELE			
Electrode gap	Plasma	Electrode thickness	Pressure
~0.05mm	Glow	0.5 mm	1 atm
~0.05mm	Glow-Arc-Glow	0.5 mm	1 atm
~0.05mm	Glow-Arc-Glow	0.5 mm	3 atm
~0.05mm	Varies	0.5 mm	3 atm(x3)
~0.05mm	Varies	0.5 mm	5 atm(x3)

5. RESULTS AND DISCUSSION

First, observe the atmospheric results. The data is structured to show the model input power in the left most plot with the thin line coupled with radiation losses shown with circles. The measured and predicted volumes are in the middle plot and the predicted temperature is in the right most plot. One goal of Figs.

9 and 10 is to show the effect of cathode fall on the results. Data for the same test is repeated twice to show the model results before and after cathode fall is removed. If the cathode fall loss is not removed as in Fig. 8a and 8c, the power added to the ignition kernel is far too large resulting in over prediction of the kernel size and radiation loss to dominate. The results where the cathode fall loss is applied (Fig. 8b and 8d) show a temperature around 6000 K which is a reasonable value when comparing to other experimental results with similar sparks events [14,16–19]. After removing the cathode fall in Fig. 8b the radiation loss becomes negligible, and the model matches the experimental volume in terms of overall data trend and the magnitude within the uncertainty of kernel volume. Two spark events are observed in Fig. 8 to show the affect arc discharge has on the measurement and model. Arc discharge is shown in results Fig. 8c and 8d

where arc discharge is the flat, discontinuous portion of the power and volume measurements. Fig. 7d shows that the spark power measurement is representative of the measured kernel volume. After applying cathode fall loss the model falls within the uncertainty of the test for the glow discharge and further the shape of the predicted volume vs time plot follows the shape of the Schlieren measured volume. Loss within the arc phase is not considered and as a result data within the arc region falls outside of the measurement uncertainty. In the following results, a loss similar in nature to the cathode fall used for the arc discharge only smaller in magnitude to the glow discharge. Further research in the arc phase should be done to experimentally determine any additional losses here for the experimental conditions presented. For now, estimations are made based on available literature.



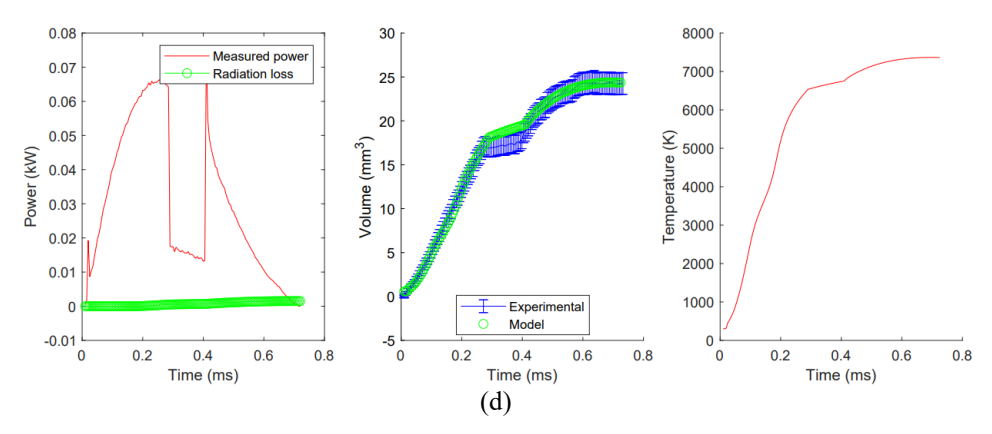
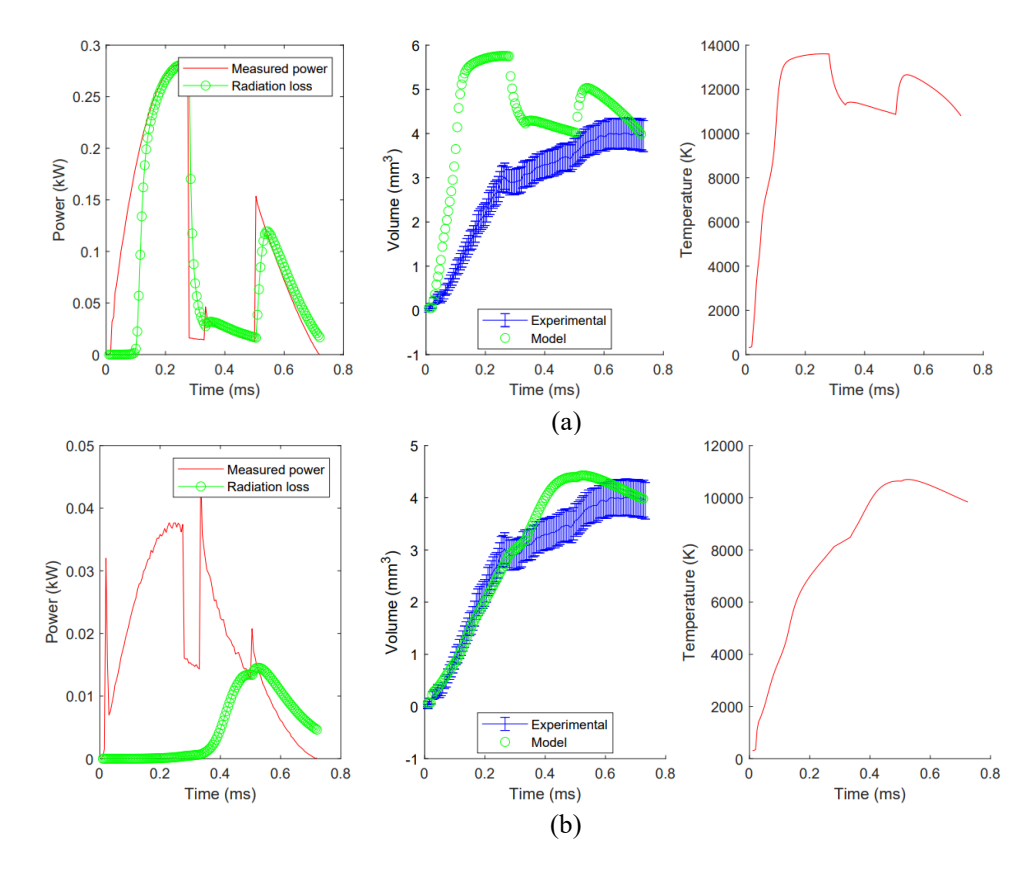


FIGURE 8: MODEL RESULTS AGAINST MEASURED KERNEL FOR AIR WITHOUT ARC DISCHARGE WITH (a) AND WITHOUT (b) CATHODE FALL ENERGY; AIR WITH ARC DISCHARGE WITH (c) AND WITHOUT (d) CATHODE FALL ENERGY

A kernel at 3 atm is presented in Fig. 9. The results are presented in a similar fashion with the cathode fall energy, and without the cathode fall energy. An additional correction is considered in Fig. 9c for the arc phase. Since the model continuously over predicts volume for the arc phase there must be some additional non-thermal loss in the arc plasma similar to the loss considered for glow discharge. The result shows that correcting by considering a cathode fall of 18 volts within the arc plasma improves accuracy of model to predict within the kernel volume uncertainty during arc discharge. Additional testing should be done to confirm the source and magnitude of the loss. It is also of interest to observe the temperature and radiation results for Fig 9c as compared to Fig. 8b and 8d. The final temperature has increased for the test at 3 atm likely because the free mean path of the current decreases resulting in higher collision rate between the electrons and heavy particles. Because of the increase in temperature the radiation has a noticeable increase over the atmospheric tests.



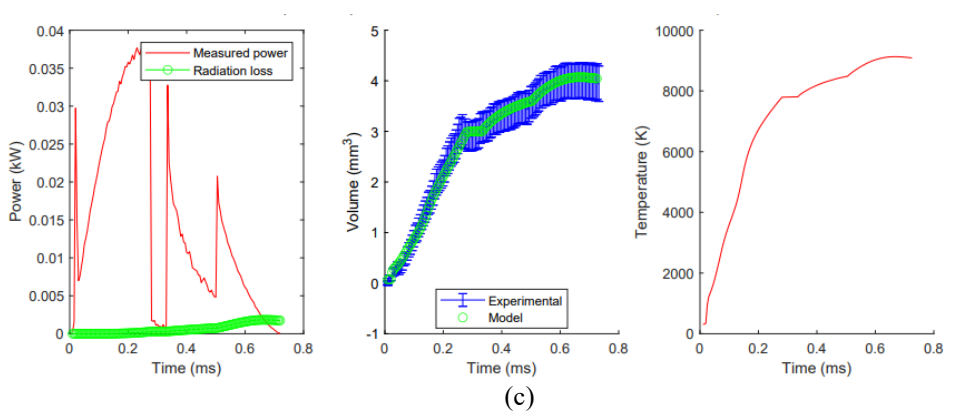
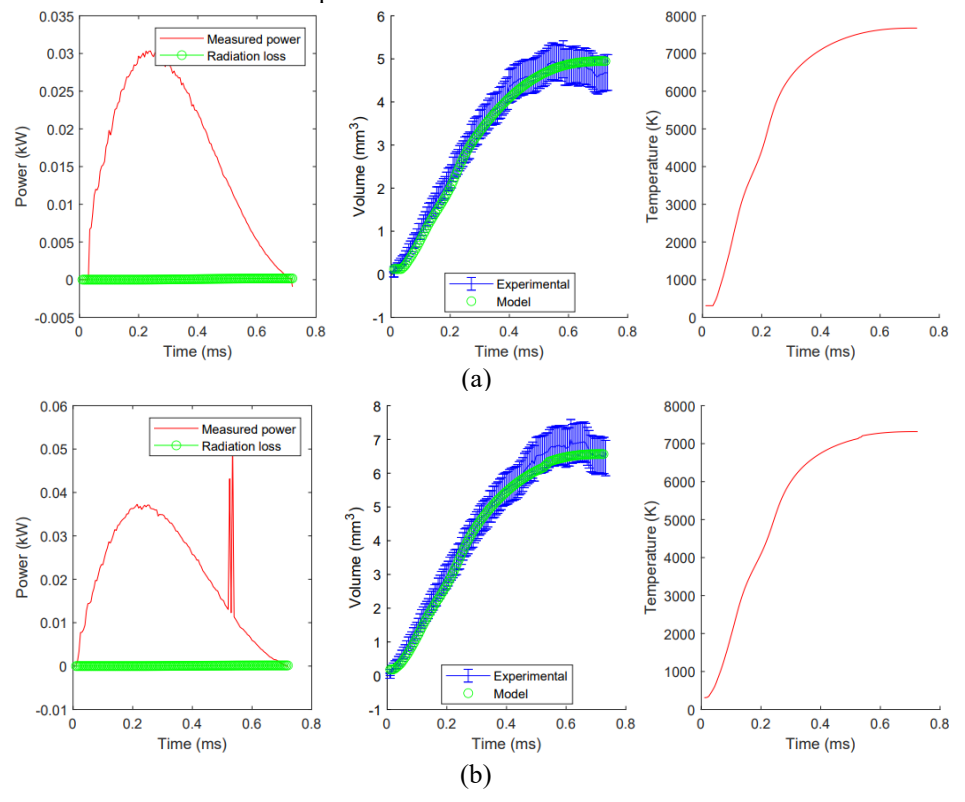


FIGURE 9: RESULTS OF MODEL FOR 3ATM (a) WITH CATHODE FALL ENERGY, (b) WITHOUT CATHODE FALL ENERGY (c) AND CATHODE FALL LOSSES WITHIN ARC PHASE ARE REMOVED.

A sample of results are presented for 3 and 5 atm air condition in Fig. 10. These results only show the fully corrected data using the cathode fall between 300V and 330V for glow discharge and an estimated loss in the arc discharge between 10V and 30V. Fig. 10a -10c represent 3 atm tests where the first two are primarily in glow discharge (Fig. 10b has short arc noise towards the end). Fig. 10c has a strong arc discharge in the second half of the spark. Again, with the full processing of the data the results fall within the measured uncertainty and the data shape follows the observed spark kernel. Tests at 5 atm is shown in Fig. 10d -10f. As the pressure increases the Schlieren kernel becomes more challenging to measure because of increased arc discharge frequency, fluid affects near the electrode and reduced kernel size. The reduction in kernel size at the end of discharge is either from radiative losses suggested in the results of the model or from the fluid affects near the electrode surface enhanced by the increased pressure. If experimental temperature measurements of the kernel were made during the testing the results could be better validated to determine if the temperature reached the values calculated in these results. Results in Fig. 10e and 10f show several strong arc pulses that greatly affect the results. With the arc pulses, especially in 10f, there can be some wrinkling in the ignition kernel surface. This wrinkling could bring into question the accuracy of the Schlieren. volume measurement however the uncertainty should encompass the possible volume change from surface effects on the kernel if the wrinkles are thinner than the width of a pixel.



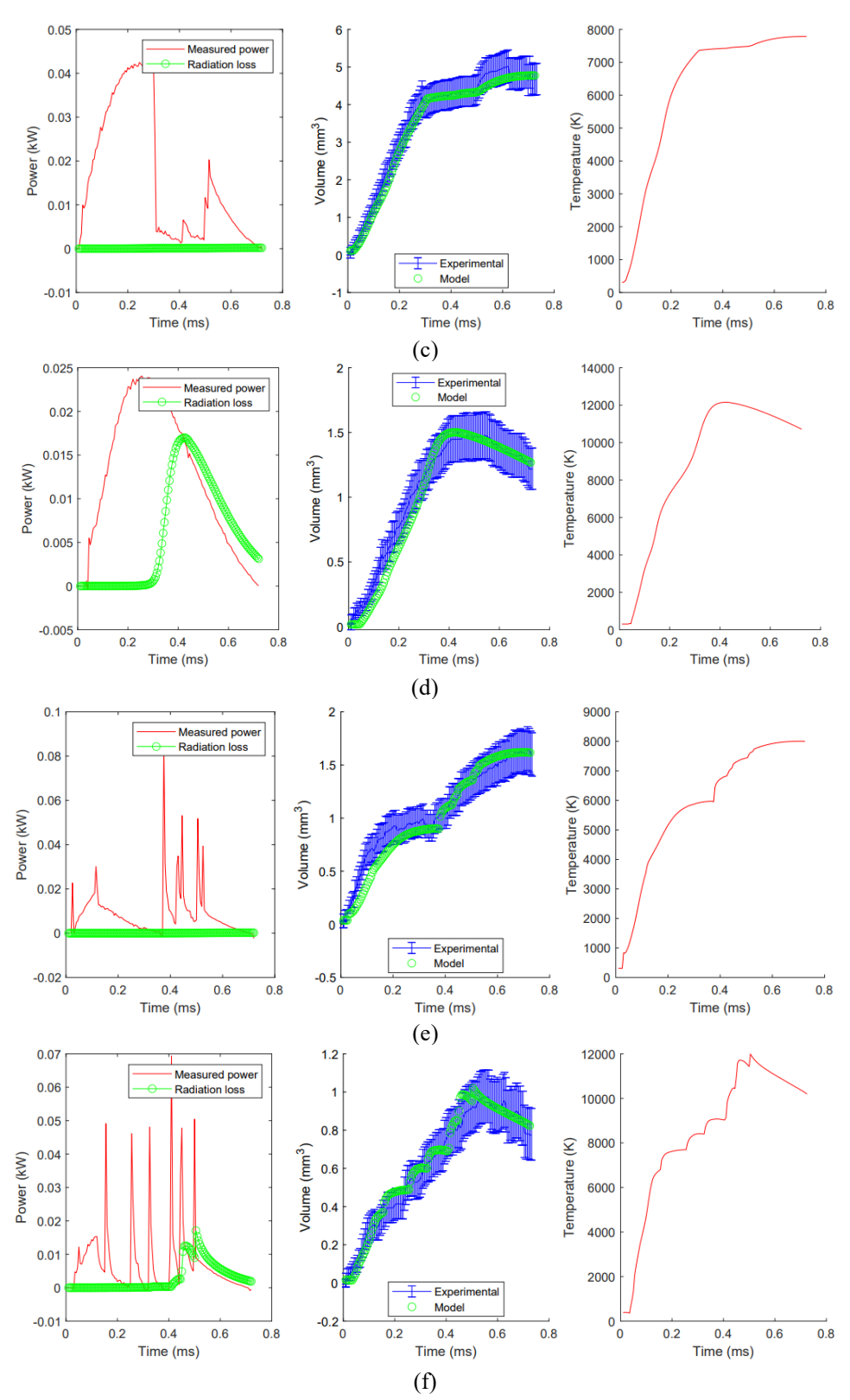


FIGURE 10: RESULTS OF MODEL FOR 3ATM WITH ALL GLOW DISCHARGE (a), (b) AND WITH ARC DISCHARGE (c). RESULTS OF MODEL FOR 5 ATM WITH ALL GLOW DISCHARGE (d) AND ARC DISCHARGE (e) AND (f).

6. CONCLUSION

The relationship between measured spark electrical power and the volume of the Schlieren kernel is provided. Results with elevated pressure for 1, 3 and 5 atm and both arc and glow plasma were observed. Using measured power, the model was able to reproduce the plot of experimental kernel volume over time. The results follow the shape of the measured kernel volume and match the magnitude of volume for a majority of the data within the stated uncertainty. Additionally, the calculated final temperature generally was found to be between 5000K and 7000K and increases with additional pressure. This temperature calculation is within reason for similar spark events that dissipate similar magnitudes of energy [14,16-19]. Removal of cathode fall energy is important for the glow discharge and after application of the model cathode fall in arc discharge was also found to be significant in the results. Further exploration into the arc discharges should be made to determine the losses mechanism, which, is likely from sheath formation within this plasma discharge regime and either needs to be measured experimentally or approximated. Additional validation of the results is desired through the measurement of average kernel temperature to ensure the model calculated temperature profile is accurate. Additionally, the thermal energy could also be measured via calorimetry to provide further validation of the suppled electrical thermal energy and further assess the accuracy of the non-thermal losses. With the relationship between the electrical power and the schlieren kernel provided in this work, future use of the model could be applied to the case with combustion and fuel present in order to calculate the affect ignition has on the radius and velocity combustion kernel. Additional work will be done with gas compositions other than air to show the affect fuels such as methane has on the results of the model and the application of this model to ignitable mixtures.

ACKNOWLEDGEMENTS

This material is based upon work supported by the National Science Foundation (NSF) under Federal Award No. CBET-2039486 issued through Combustion and Fire System (CFS) program.

REFERENCES

- [1] Al-Shahrany, A. S., Bradley, D., Lawes, M., and Woolley, R., 2005, "Measurement of Unstable Burning Velocities of Iso-Octane-Air Mixtures at High Pressure and the Derivation of Laminar Burning Velocities," Proc. Combust. Inst., **30**(1), pp. 225–232. DOI 10.1016/j.proci.2004.07.044.
- [2] Kim, J., and Anderson, R. W., 1995, "Spark Anemometry of Bulk Gas Velocity at the Plug Gap of a Firing Engine," *SAE Technical Papers*, SAE International.
- [3] Sher, E., Ben-Ya'Ish, J., and Kravchik, T., 1992, "On the Birth of Spark Channels," Combust. Flame, **89**(2), pp. 186–194. DOI 10.1016/0010-2180(92)90027-M.
- [4] Venkattraman, A., 2013, "Cathode Fall Model and Current-Voltage Characteristics of Field Emission Driven Direct Current Microplasmas," Phys. Plasmas, **20**(11), p. 113505. DOI 10.1063/1.4829680.
- [5] Kolobov, V. I., and Tsendin, L. D., 1992, "Analytic Model of the Cathode Region of a Short Glow Discharge in Light Gases,"

- Phys. Rev. A, **46**(12), pp. 7837–7852. DOI 10.1103/PhysRevA.46.7837.
- [6] Sommerer, T. J., Hitchon, W. N. G., and Lawler, J. E., 1989, "Self-Consistent Kinetic Model of the Cathode Fall of a Glow Discharge," Phys. Rev. A, **39**(12), pp. 6356–6366. DOI 10.1103/PhysRevA.39.6356.
- [7] Kaur, J., and Kant, R., 2017, "Theory of Work Function and Potential of Zero Charge for Metal Nanostructured and Rough Electrodes," J. Phys. Chem. C, **121**(24), pp. 13059–13069. DOI 10.1021/acs.jpcc.7b03595.
- [8] Hao, Y., Zheng, B., and Liu, Y., 2013, "Cathode Fall Measurement in a Dielectric Barrier Discharge in Helium," Phys. Plasmas, **20**(11). DOI 10.1063/1.4834515.
- [9] Uhrlandt, D., Baeva, M., Pipa, A. V, Kozakov, R., and Gött, G., 2015, "Cathode Fall Voltage of TIG Arcs from a Non-Equilibrium Arc Model," Weld. World, **59**(1), pp. 127–135. DOI 10.1007/s40194-014-0188-x.
- [10] Maly, R., 1981, "Ignition Model for Spark Discharges and the Early Phase of Flame Front Growth," Symp. Combust., **18**(1), pp. 1747–1754. DOI 10.1016/S0082-0784(81)80179-8.
- [11] Billoux, T., Cressault, Y., Teulet, P., and Gleizes, A., 2012, "Calculation of the Net Emission Coefficient of an Air Thermal Plasma at Very High Pressure," *Journal of Physics: Conference Series*.
- [12] Askari, O., 2018, "Thermodynamic Properties of Pure and Mixed Thermal Plasmas Over a Wide Range of Temperature and Pressure," J. Energy Resour. Technol. Trans. ASME, **140**(3). DOI 10.1115/1.4037688.
- [13] Askari, O., Beretta, G. P., Eisazadeh-Far, K., and Metghalchi, H., 2016, "On the Thermodynamic Properties of Thermal Plasma in the Flame Kernel of Hydrocarbon/Air Premixed Gases," Eur. Phys. J. D, **70**(8), p. 159. DOI 10.1140/epjd/e2016-70195-4.
- [14] Kawahara, N., Watanabe, M., Tomita, E., Nagano, Y., and Kitagawa, T., 2019, "Plasma Temperature of Spark Discharge in a Lean-Burn Spark-Ignition Engine Using a Time Series of Spectra Measurements," *SAE Technical Papers*, pp. 4–7.
- [15] Lichtenberg, S., Dabringhausen, L., Langenscheidt, O., and Mentel, J., 2005, "The Plasma Boundary Layer of HID-Cathodes: Modelling and Numerical Results," *Journal of Physics D: Applied Physics*, pp. 3112–3127.
- [16] Wang, J., He, M., Zheng, P., Chen, Y., and Mao, X., 2019, "Comparison of the Plasma Temperature and Electron Number Density of the Pulsed Electrolyte Cathode Atmospheric Pressure Discharge and the Direct Current Solution Cathode Glow Discharge," Anal. Lett., **52**(4), pp. 697–712. DOI 10.1080/00032719.2018.1487449.
- [17] Ono, R., Nifuku, M., Fujiwara, S., Horiguchi, S., and Oda, T., 2005, "Gas Temperature of Capacitance Spark Discharge in Air," J. Appl. Phys., **97**(12), p. 123307. DOI 10.1063/1.1938274.
- [18] Benilov, M. S., Benilova, L. G., Li, H. P., and Wu, G. Q., 2012, "Sheath and Arc-Column Voltages in High-Pressure Arc Discharges," J. Phys. D. Appl. Phys., **45**(35), p. 10. DOI 10.1088/0022-3727/45/35/355201.
- [19] Staack, D., Farouk, B., Gutsol, A. F., and Fridman, A., 2007, "Spatially Resolved Temperature Measurements of Atmospheric-Pressure Normal Glow Microplasmas in Air," IEEE Trans. Plasma Sci., **35**(5 II), pp. 1448–1455. DOI 10.1109/TPS.2007.904959.